European Journal of Pharmaceutics and Biopharmaceutics 201 (2024) 114354

Contents lists available at ScienceDirect

European Journal of Pharmaceutics and Biopharmaceutics

journal homepage: www.elsevier.com/locate/ejpb

Aptamer-Drug conjugates for a targeted and synergistic anticancer Response: Exploiting T30923-5-fluoro-2′-deoxyuridine (INT-FdU) derivatives

Daniela Benigno [a,1], Natalia Navarro [b,c,1], Anna Aviñó [b,c], Veronica Esposito [a], Aldo Galeone [a], Antonella Virgilio [a,*], Carme Fàbrega [b,c,**], Ramon Eritja [b,c,***]

[a] Department of Pharmacy, University of Naples Federico II, Napoli 80131, Italy
[b] Nucleic Acids Chemistry Group, Institute for Advanced Chemistry of Catalonia (IQAC-CSIC), Barcelona 08034, Spain
[c] Nucleic Acids Chemistry Group, Networking Center on Bioengineering, Biomaterials and Nanomedicine (CIBER-BBN), Barcelona 08034, Spain

ARTICLE INFO

Keywords:
Aptamer-drug
5-fluoro-2′-deoxyuridine
G-quadruplex
T30923 aptamer
Cancer therapy

ABSTRACT

One of the most appealing approaches for cancer treatment is targeted therapy, which is based on the use of drugs able to target cancer cells without affecting normal ones. This strategy lets to overcome the major limitation of conventional chemotherapy, namely the lack of specificity of anticancer drugs, which often leads to severe side effects, decreasing the therapy effectiveness. Delivery of cell-killing substances to tumor cells is one-way targeted drug therapy can work. Generally, monoclonal antibodies are combined with chemotherapeutic drugs, allowing cellular uptake through the binding to their targets on the surface of cancer cells. Aptamer-drug conjugates represent a promising alternative solution to antibodies to minimize off-target effects, considering the remarkable selective binding capabilities of aptamers. In this study, to enhance the therapeutic efficacy of the antineoplastic agent 5-fluoro-2′-deoxyuridine (FdU) in various cancer cells, we focused on the development of a novel conjugate using the antiproliferative aptamer T30923 (INT) as a drug vehicle. Three derivatives composed of T30923 conjugated with a different number of FdU units were synthesized, and their structural and biological properties were thoroughly characterized, highlighting their potential for targeted and synergistic anticancer responses.

1. Introduction

Targeted drug delivery within tumor-specific sites has garnered significant interest in cancer therapy because of the life-threatening toxic effects often associated with the lack of specificity in conventional chemotherapy. In recent years, considerable efforts have been devoted to delivering cell-killing substances to tumor cells without harming the rest of the organism. For this reason, ligand-drug conjugates such as antibodies, lipids, peptides, small molecules, and aptamers have been designed to increase selectivity and reduce off-target effects [1].

Therapeutic nucleoside and nucleobase analogs represent an attractive class of antineoplastic drug candidates. Among them, 5-fluorouracil (5-FU) and 5-fluoro-2′-deoxyuridine (floxuridine, FdU) have been widely used in various cancer types with proven efficacy [2]. FdU, in particular, has been evaluated as an alternative to 5-FU proving increasing cytotoxic activity [3].

Despite its advantages, the clinical utility of FdU has been hindered by its short half-life in vivo, uncertain drug resistance, and, most significantly, its non-selective targeting, affecting both tumor and normal cells [4]. In recent years, several approaches have been developed to tackle these challenges, including its incorporation into DNA nanostructures [5,6] and its conjugation to lipids or proteins [7,8].

* Corresponding author at: Department of Pharmacy, University of Naples Federico II, Napoli, 80131, Italy.
** Corresponding author at: Nucleic Acids Chemistry Group, Institute for Advanced Chemistry of Catalonia (IQAC-CSIC) and Networking Center on Bioengineering, Biomaterials and Nanomedicine (CIBER-BBN), Barcelona, 08034, Spain.
*** Corresponding author at: Nucleic Acids Chemistry Group, Institute for Advanced Chemistry of Catalonia (IQAC-CSIC) and Networking Center on Bioengineering, Biomaterials and Nanomedicine (CIBER-BBN), Barcelona, 08034, Spain.
E-mail addresses: antonella.virgilio@unina.it (A. Virgilio), carme.fabrega@iqac.csic.es (C. Fàbrega), recgma@cid.csic.es (R. Eritja).
[1] These authors contributed equally to this work.

https://doi.org/10.1016/j.ejpb.2024.114354
Received 26 March 2024; Received in revised form 29 May 2024; Accepted 7 June 2024
Available online 7 June 2024

A novel alternative strategy, that has shown promise in minimizing the side effects of nucleotide analog drugs, involves the development of aptamers intrinsically comprised of various units of 5-fluoro-2′-deoxyuridine [9,10] or aptamer-FdU conjugates [11–13]. Aptamers, also known as "chemical antibodies", are an innovative class of molecules selected from a library of DNA or RNA sequences by a process called SELEX (Systematic Evolution of Ligands by Exponential Enrichment) [14]. These molecules are artificial single-chain DNA or RNA oligonucleotides typically 20- to 80-nucleotides-long, that can adopt distinctive three-dimensional structures and recognize and bind their targets with high affinity and specificity [15]. Aptamers not only have the advantages of antibodies, such as high affinity, excellent specificity, and low toxicity and immunogenicity, but they are also stable and easy to synthesize, modify, and manipulate [16]. Due to their targeting properties and high specificity for different types of tumor cells, aptamer-drug conjugates (ApDCs) have demonstrated several advantages in enhancing the efficacy of numerous conventional antitumor drugs [17].

A significant subset of aptamers, characterized by G-rich sequences, adopts G-quadruplex structures (G4s) [18]. G4 structures, composed of planar squared arrangements of four guanines (G-tetrads) interconnected by eight Hoogsteen hydrogen bonds and stabilized by cations accommodated in their central cavity, offer outstanding polymorphism and stability [19,20]. G-quadruplexes naturally occur in specific human genomic regions, such as telomeres and promoters, participating in several cellular processes, making them interesting molecular targets for drugs [21]. Additionally, as aptamer scaffolds, certain exogenous G4 structures can interact with a wide variety of biological targets. These properties make G4 aptamers a highly investigated class of compounds for therapeutic purposes.

Recent advances in anticancer agents have highlighted the potential of G4-aptamers in clinical applications [22]. Several G4-forming sequences have exhibited remarkable antiproliferative properties against various types of cancer cells, suggesting that this biological property may be a general characteristic of G-rich ODNs [23]. Among these, the nucleolin-targeting aptamer AS1411 has proven particularly promising, showing encouraging results in phase 2b clinical trials for acute myeloid leukemia and renal cell carcinoma [24]. T40214 (STAT) and a newly discovered closely related structure, STATB [25,26], have also demonstrated antiproliferative activity by modulating the STAT3 pathway, frequently activated in many human cancers.

Another noteworthy G4-aptamer is T30923 (INT), which is able to bind to the HIV-1 integrase (HIV-IN), thus showing remarkable antiviral activity [27–29]. INT has also demonstrated a high affinity for another protein, the interleukin-6 receptor (IL-6R) which, in turn, activates STAT3 [30]. Furthermore, several studies have indicated that this aptamer possesses interesting anticancer properties [23,31,32]. Particularly, a thorough screening of six different tumor cell lines has proved that INT consistently inhibits cell proliferation in all tested tumor cell lines in a time- and dose-dependent manner [33]. INT sequence folds into a head-to-head 5′-5′ dimer composed by the stacking of two identical parallel G4 structures, each formed by three G-tetrads and three propeller loops, consisting of only one thymidine [34].

Recently, parallel tetramolecular quadruplexes have been used to enhance the transport of the FdU in FU-resistant colorectal cancer cells [35]. Furthermore, to overcome the drawbacks associated with the use of 5-FU and FdU, an oligomer consisting of 10 units of FdUMP (5-fluoro-2′-deoxyuridylate) nucleotides serially connected, was designed. This construct can generate floxuridine monophosphate inside cells after nuclease digestion and exhibits higher cytotoxicity than conventional fluoropyrimidine drugs against proliferating malignant cells by a unique mechanism that involves dual targeting of thymidylate synthase and Top1 [36]. However, this system did not prove non-specificity for normal cells.

With the aim to explore a novel drug delivery vehicle for 5-fluoro-2′-deoxyuridine (floxuridine, FdU), a different number of FdU units has been conjugated to the T30923 (INT) aptamer sequence. This strategy seeks to enhance the efficiency of FdU, eliciting a targeted and synergistic anticancer response in multiple cancer cell types. To this end, T30923 conjugated with one, five, or ten units of FdU at the 3′ ends was synthesized. We thoroughly analyzed the structural and biological properties of the conjugates in comparison to the parent sequence INT, the drug oligomers (FdU_5 and FdU_{10}) alone and the sequence INT-T_{10}, containing a 10mer-thymidine tail at the 3′ end of INT, used as a reference of an INT/not-drug oligomer conjugated system (Fig. 1 and Table 1).

2. Material and methods

2.1. Synthesis and characterization of the oligonucleotides

All the oligonucleotide sequences detailed in Table 1 were synthesized on an H-8 DNA synthesizer (K&A Laboratories, Germany) at the 1 μmol scale (CPG synthesis) using standard DMT-off protocols. FdU phosphoramidites and Fluorescein (FAM) were positioned at the 3′ end of the sequences. The oligomers were detached from the support and deprotected by treatment with concentrated aqueous ammonia (32 %) overnight, followed by 1 h at 55 °C and subsequently desalted using a NAP-10 column (GE Healthcare, Little Chalfont, UK). The length and homogeneity of the oligonucleotides were checked by HPLC (Supplementary Fig. S1, S2, S3, S4, S5), on a Nucleogel SAX column (Macherey-Nagel, 1000–8/46) using buffer A (20 mM NaH_2PO_4/Na_2HPO_4 aqueous solution (pH 7.0) containing 20 % (v/v) CH_3CN) and buffer B (1 M NaCl, 20 mM NaH_2PO_4/Na_2HPO_4 aqueous solution (pH 7.0) containing 20 % (v/v) CH3CN); a linear gradient from 0 % to 100 % B for 45 min and a flow rate of 1 mL/min were used. The isolated oligomers proved to be > 98 % pure by NMR and the expected mass was confirmed by MALDI-TOF (Table 1, Supplementary Fig. S6, S7, S8, S9, S10, S11, S12, S13).

2.2. NMR spectroscopy

NMR samples were prepared at a concentration of approximately 1 mM in 0.2 mL (H2O/D2O 9:1 v/v) of buffer solution with 10 mM KH_2PO_4/K_2HPO_4, 70 mM KCl, and 0.2 mM EDTA (pH 7.0). All the samples were heated for 5–10 min at 90 °C and slowly cooled (10–12 h) to room temperature. The solutions were equilibrated for several hours at 4 °C. The annealing process was assumed to be complete when the ^1H NMR spectra were superimposable on changing time. NMR spectra were recorded at 25 °C by employing a 700 MHz Bruker spectrometer (Bruker-Biospin, Billerica, Massachusetts, US). Proton chemical shifts were referenced to the residual water signal, resonating at 4.78 ppm (25 °C, pH 7.0). Water suppression was achieved using the excitation sculpting with the gradient routine included in the "zgesgp" pulse sequence [37]. NMR data processing was done by using the vendor software TOPSPIN 4.1.4 (Bruker Biospin Gmbh, Rheinstetten, Germany).

2.3. Circular dichroism spectroscopy

CD samples of INT and its conjugated derivatives were prepared at a concentration of 3 μM using either a potassium phosphate buffer (10 mM KH_2PO_4/K_2HPO_4, 70 mM KCl, pH 7.0) or a sodium phosphate buffer (10 mM NaH_2PO_4/Na_2HPO_4, 5 mM NaCl, pH 7.0) and submitted to the annealing procedure (heating at 90 °C and slowly cooling at room temperature). All quadruplexes' CD spectra and melting curves were recorded on a Jasco 1500CD spectrophotometer at 20 °C with the temperature maintained constant using a thermoelectrically controlled cell holder (Jasco PTC-517). The spectra were obtained over a range of 220–320 nm with a scanning speed of 100 nm/min, a response time of 4 s, a 0.1-nm data pitch, and normalized by subtraction of the background scan with the potassium or sodium buffer.

CD melting curves were registered as a function of temperature (20–95 °C) for all quadruplexes at their maximum Cotton effect

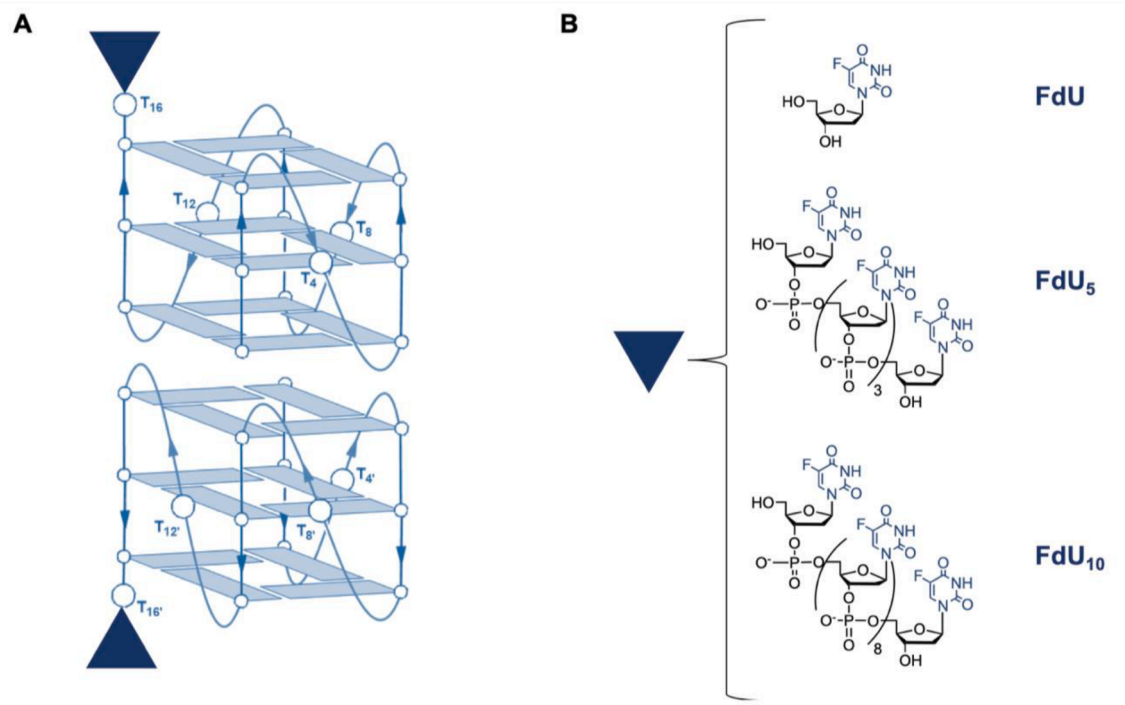

Fig. 1. (A) Schematic representation of the G4 structures adopted by the conjugated INT/FdU sequences studied. The large circles represent the thymidines, small circles represent the guanosines, and triangles represent floxuridine (FdU) oligomers. (B) Chemical structures of FdU oligomers composed of one, five, and ten monomer units.

Table 1
Sequences, melting temperatures in sodium buffer (Tm) and MALDI-TOF characterizations of the investigated ODNs. Expected (exp) and found (f) molecular weights are listed for comparison.

Name	Sequences	MWf	MWexp	Tm (°C) ± 1
INT	GGGTGGGTGGGTGGGT	5094	5102	60 °C
INT-FdU	GGGTGGGTGGGTGGGT-(FdU)	5403	5411	59 °C
INT-FdU_5	GGGTGGGTGGGTGGGT-$(FdU)_5$	6634	6647	55 °C
INT-FdU_{10}	GGGTGGGTGGGTGGGT-$(FdU)_{10}$	8195	8192	52 °C
INT-T_{10}	GGGTGGGTGGGTGGGT-$(T)_{10}$	8144	8142	53 °C
FdU_5	$(FdU)_5$	1477	1479	—
FdU_{10}	$(FdU)_{10}$	3017	3017	—
T_{10}	$(T)_{10}$	2978	2978	—

wavelengths. The data were recorded in a 1 cm pathlength cuvette with a scan rate of 30 °C/h. The melting temperature (Tm) values provided the best fit of the experimental melting data.

2.4. Polyacrylamide gel electrophoresis (PAGE)

All oligonucleotides were analyzed by polyacrylamide gel electrophoresis (PAGE) under native conditions. All oligonucleotide samples were prepared at the same concentration of 1 mM in potassium phosphate buffer and underwent the annealing procedure as described previously. For all samples, a solution of glycerol/TBE 10 × was added just before loading. Each sample was loaded onto a 15 % polyacrylamide gel containing TBE 2.5 × and 20 mM KCl. The running buffer was TBE 1 × supplemented with 50 mM KCl. Electrophoresis was carried out at 100 V/cm, for at least 1 h at 20 °C. Subsequently, bands were visualized by staining with Stains-All (Sigma-Aldrich, Madrid, Spain).

2.5. Nuclease degradation assay

Nuclease stability assay of modified oligonucleotides was conducted in a 10 % fetal bovine serum (FBS) solution diluted with Dulbecco's Modified Eagle's Medium (DMEM) at 37 °C. Approximately 6 nmol of stock solution of each ODN was evaporated to dryness under reduced pressure and then incubated with 200 µl 10 % FBS at 37 °C. At 0, 24 and 48, 50 µl of samples were collected and stored at –20 °C for at least 20 min. Subsequently, the samples were dried, and 5 µl of gel loading buffer consisting of glycerol/TBE 10 × was added. PAGE was carried out at room temperature using a 20 % polyacrylamide gel in 1 × TBE buffer. The patterns on the gel were visualized by UV shadowing.

2.6. Cell culture

HeLa and HCC2998 cells were purchased from the American Type Culture Collection (Manassas, VA, USA). HCT116 and Fibroblasts cells were kindly provided by IQAC, Barcelona, Spain. All cell lines were maintained in high-glucose DMEM supplemented with 10 % FBS. The cells were cultured at 37 °C, 5 % CO2 and were routinely tested for mycoplasma contamination.

2.7. Internalization by flow cytometry

To investigate the internalization of INT-FdU_{10} and its corresponding control sequences, cells were initially seeded at a density of 80,000 cells per well in 24-well plates. On the following day, samples labeled with FAM were dissolved in fresh medium, resulting in a final 1 µM concentration, and incubated for 24 h. Then, cells were washed with PBS, followed by harvesting through trypsin treatment. After harvesting, the cells were taken up in cell culture and centrifuged at 1,000 rpm for 8 min. This process was repeated twice, and the remaining supernatant was resuspended in cold PBS. Two independent experiments were conducted, and each condition was measured in duplicate.

2.8. Internalization pathway studies

Cells were seeded at a density of 80,000 cells per well within 24-well plates. The next day, to inhibit specific endocytic pathways, cells were

pretreated separately as follows: 0.25 μM, Cytochalasin D (to inhibit phagocytosis and macropinocytosis) for 15 min, 625 nM Methyl-β-Cyclodextrin (to inhibit caveolin-dependent endocytosis) for 30 min, or 100 nM sucrose (to inhibit clathrin-dependent endocytosis) for 30 min.

Following these pretreatments, 1 μM of every oligonucleotide was added in a final volume of 500 μl and incubated for 24 h. Subsequently, the cells were washed with PBS, harvested through trypsin treatment, suspended in cell culture medium, and centrifuged at 1,000 rpm for 5 min. This process was repeated twice using PBS, and the remaining supernatant was resuspended in cold PBS. Two independent experiments were conducted, and each experiment was performed in duplicate.

2.9. Fluorescence microscopy

For fluorescence microscopy studies, cells were first seeded the day before at a density of 2,500 cells per well. Then, samples were incubated at a concentration of 1 μM for 24 h. Following the incubation period, the cells underwent a PBS wash. To fix the cells, a 4 % paraformaldehyde solution was employed, and the nuclei were stained using DAPI. Image analysis was performed using ImageJ (U. S. National Institutes of Health, Bethesda, Maryland, USA). The fluorescence microscopy images presented are representative of the many images acquired during the experiments.

2.10. Cell proliferation assay (MTT)

The cytotoxicity of the prepared oligonucleotides was evaluated using the MTT (1-(4,5-dimethylthiazol-2-yl)-3,5-diphenylformazan) assay. Cells were seeded at a density of 5,000 cells per well in 96-well plates and allowed to culture overnight. Subsequently, samples at different concentrations (500 nM, 1 μM, and 5 μM) were added and incubated for 48 h. Following this incubation period, cells were washed with PBS and MTT reagent was added to each well, resulting in a final concentration of 0.5 mg/mL. After 2 h of incubation, the medium was carefully removed, and formazan crystals were dissolved by the addition of DMSO. Absorbance values were subsequently measured at 570 nm. This experiment was repeated independently three times, each time in triplicate and the data was normalized to the value of untreated cells (100 % viability).

2.11. Statistical analysis

Statistical analysis was conducted using GraphPad Prism 8 (GraphPad Software, Inc., La Jolla, CA, USA). The quantified data is expressed as the mean ± standard deviation (SD). To assess statistical differences, a one-way ANOVA with the Tukey post hoc test was employed, with significance levels indicated as follows: (*$p \leq 0.0332$, **$p \leq 0.0021$, ***$p \leq 0.0002$, **** $p \leq 0.0001$).

3. Results and discussion

To evaluate the synergistic anticancer effects, produced by the conjugation of T30923 with a different number of FdU residues, a series of oligodeoxynucleotides (ODN) was prepared by solid-phase phosphoramidite chemistry and their purity was checked by HPLC (Supplementary Fig. S1, S2, S3, S4, S5). The ODN sequences, melting temperatures in sodium buffer and mass spectrometry characterization data are listed in Table 1 and in Supplementary Fig S6, S7, S8, S9, S10, S11, S12 and S13.

3.1. NMR spectroscopy

To confirm the ability of the conjugated G-rich ODNs reported in Table 1 to preserve the characteristic G4 folded structure of INT, despite the presence of a variable number of FdU units at the 3′ ends, the samples, properly annealed, were analyzed by ^{1}H NMR and compared with the parent INT sequence (Fig. 2 and Supplementary Fig. S14). The imino proton regions (10.5–12.0 ppm) diagnostic of the presence of G-quadruplexes are almost superimposable, indicating that the presence of a variable number of FdU or T units at the 3′ end of the INT sequence does not prevent INT from adopting its typical G-quadruplex structure. In particular, the close similarity of the imino regions of all ^{1}H NMR spectra confirms that all conjugates maintain unaffected the INT capacity to fold in 5′-5′ end-to-end staked dimers of parallel G-quadruplexes. Instead, the presence of unstructured 3′ end tails constituted by a different number of monomers is confirmed by a major complexity of the aromatic region signals of the conjugates compared to that of INT (Supplementary Fig. S14).

3.2. Circular dichroism spectroscopy

The ability of all conjugated ODNs to fold into parallel G-quadruplex structures similar to INT was also evaluated using circular dichroism (CD) (Fig. 3). Most of the conjugated derivatives exhibited CD profiles nearly identical to that of the parent sequence and comparable to each other. Specifically, they displayed a minor negative band at 242 nm and a major positive band at 263 nm, characteristic of a parallel folding pattern where all guanosines adopt anti-glycosidic conformations. Only the long-tailed conjugates, INT-FdU_{10} and INT-T_{10}, showed slight differences in their CD spectra, particularly in the region between 270 and 300 nm, while both retained the typical profile of parallel G-quadruplexes.

3.3. Melting denaturation analysis by circular dichroism

To evaluate the effect of varying numbers of FdU units on the thermal stability of these structures, CD thermal denaturation experiments were performed using a potassium phosphate buffer (10 mM KH_2PO_4/K_2HPO_4, 70 mM KCl, pH 7.0). The heating curves for all sequences indicated that the melting process starts around 80 °C, suggesting that the different tails do not dramatically influence the G4 thermal stability (Supplementary Fig. S15). These data clearly indicate that under biological assay conditions (37 °C) all G4 structures exhibit remarkable stability. Furthermore, to obtain well-defined sigmoidal CD heating profiles of INT-FdU derivatives and determine their melting temperatures (Tm), CD experiments for all samples were conducted at very low sodium ion concentrations (10 mM NaH_2PO_4/Na_2HPO_4, 5 mM NaCl, pH 7.0) (Supplementary Fig. S16, S17). Under these conditions, all conjugated derivatives showed a lower Tm than that of INT, although not to a

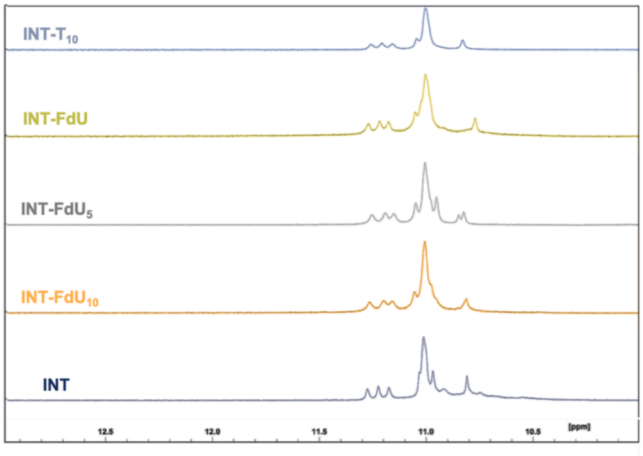

Fig. 2. Imino proton regions of the ^{1}H NMR spectra (700 MHz) of the investigated ODNs.

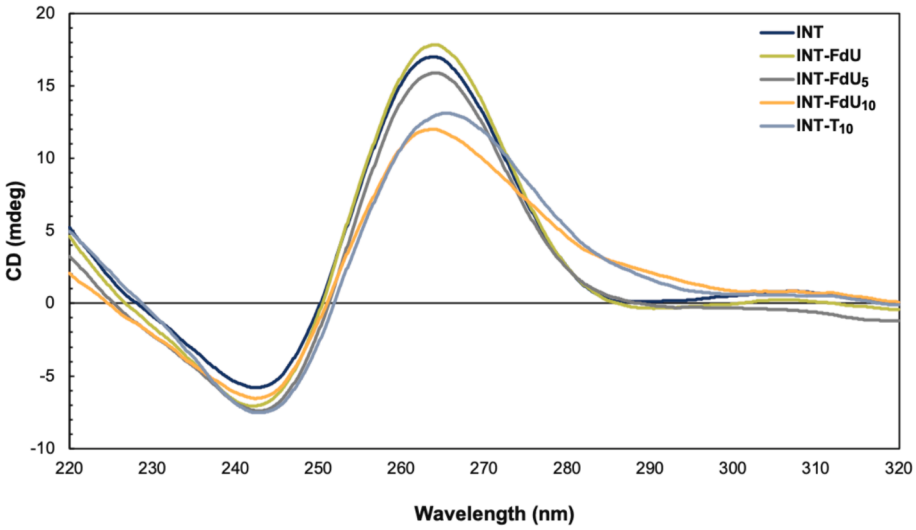

Fig. 3. Circular Dichroism spectra of the investigated ODNs at 20 °C in a potassium phosphate buffer.

drastic extent.

3.4. Polyacrylamide gel electrophoresis (PAGE)

It has been previously reported that the INT aptamer folds into a dimeric parallel-stranded G4 structure [34]. Polyacrylamide gel electrophoretic techniques provide information about the molecular sizes and molecularity of complexes, especially when studying monomer–dimer equilibrium. To confirm the ability of INT conjugates to form dimers, all investigated G-quadruplexes were studied by 15 % native polyacrylamide gel electrophoresis (PAGE) in the presence of 50 mM KCl (Supplementary Fig. S18). In all G4 samples, a predominant slower-migrating band, characteristic of dimeric structures, was observed, with retardation in gel mobility as G-quadruplex structure size increased. The PAGE results confirm the presence of dimeric G4 structures in the modified sequences, strictly resembling the structure adopted by the parent ODN, consistent with the NMR and CD data.

3.5. Nuclease stability assay

The resistance of the designed INT-FdU_n conjugates in biological environments was evaluated through a degradation assay in 10 % fresh fetal bovine serum (FBS) at 37 °C followed by gel electrophoresis analysis. The ODNs resistance was evaluated during the same range of time as the MTT assays evaluating cell viability, which were conducted up to 48 h. Importantly, according to previous studies [33], under these conditions, INT showed remarkable stability to serum nucleases being resistant for up to 48 h under these conditions. The electrophoretic profiles indicated that the aptamer-drug conjugates underwent the complete degradation of the entire oligomeric tail into FdU monomers already at 24 h, since in all cases at both 24 and 48 h only the fastest migrating band corresponding to the stable INT quadruplex persisted (Supplementary Fig. S19). These data are very interesting for evaluating the pharmacological potential of these INT-FdU conjugates, since, as previously reported, oligomeric FdU exerts its cytotoxic activity by undergoing oligomer degradation through nucleases, resulting in the production of FdU and FdUMP [36]. The exceptional resistance of INT in the biological environment ensures the synergistic effect of G-quadruplex and drug conjugation even up to 48 h. These results suggest that following endocytosis, INT-FdU_n conjugates trafficked to the lysosomes and underwent degradation to release the active therapeutic compound. At this stage, the oligomeric FdU prodrug becomes active, while the INT structure, having shed all FdU units, remains intact, allowing it to sustain its cytotoxic activity.

3.6. Antitumor synergy of INT-FdU_n conjugates

While there has been an improvement in response rates and disease-free survival across various types of cancers, the most significant impact of 5-FU and FdU has been reported in colorectal cancer (CRC). In light of this, for the cellular studies, we selected two colorectal cancer cell lines, HCT116 and HCC2998, which have different sensitivity levels to 5-FU, with the latter demonstrating higher resistance [38]. Additionally, to broaden the scope of our research to another type of cancer, we extended our investigations to HeLa cells. Finally, a healthy non-tumor cell line named Fibroblasts was studied. We explored the antitumor activity of INT-FdU_n conjugates on cell proliferation by conducting the MTT assay (Fig. 4). Cells were treated with three different concentrations of oligonucleotides (0.5, 1, and 5 μM) over 48 h.

Our findings indicated that by increasing the number of FdU units added to the 3′ end of INT, the cytotoxic activity of conjugates, against all cancer cell lines and at all concentrations, is enhanced compared to the not conjugated sequence, INT. Notably, in almost all cases, INT-FdU_n outperformed the bare oligomeric forms of FdU (FdU_5 and FdU_{10}). INT-FdU_{10} exhibited the highest level of antiproliferative activity, resulting in the most substantial reduction in the percentage of viable cells. At the highest concentration, viability in both HCT116 and HeLa cells was significantly reduced by 65 %. In HCC2998, treatment with nucleobase drugs alone led to only a 20 % inhibition, as anticipated, highlighting its resistance and the different sensitivity to FdU between the two studied colorectal cancer cell lines. Meanwhile, conjugation with INT effectively diminished the growth rate in these cancer cells (a 50 % decrease with INT-FdU_{10} at approximately 5 μM), circumventing the resistance observed in HCC2998. These results indicate that the studied aptamer-drug conjugates truly possess enhanced cytotoxicity toward cancer cells. Moreover, the cytotoxicity of INT-T_{10} and T_{10} was also evaluated in all cell lines, resulting in almost 100 % of viability (Supplementary Fig. S20, S21, S22, S23). In a previous study [33], we demonstrated that at 10 μM and 50 μM, INT can develop antitumor activity in certain cancer cell lines. It is important to highlight that in this case, by acting synergistically, INT and FdU oligomers, are able to achieve antitumor activity in the range of 500 nM and 5 μM.

Finally, the targeting efficacy of the aptamer was assessed on healthy human fibroblast cells. FdU_5 and FdU_{10} inhibited fibroblast cell growth by 65 % and 70 %, respectively, demonstrating a lack of specificity for cancer cells. Cell viability values of 80 % for INT-FdU_5 and 70 % for INT-FdU_{10} were observed, halving the cell death caused by oligomeric drugs alone. These data confirm that the coexistence of INT and $(FdU)_n$ not only strengthens the killing effect of free FdU by a synergistic effect, but

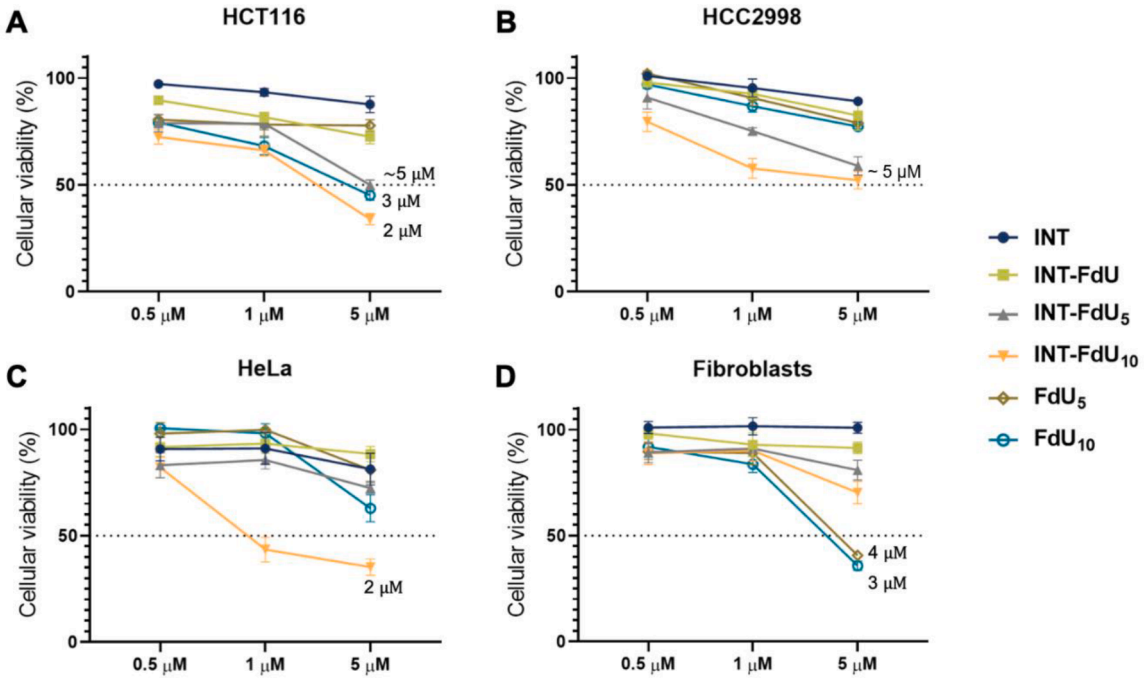

Fig. 4. Cellular viability studies after 48 h determined by MTT assay. Three different concentrations (0.5 μM, 1 μM and 5 μM) of INT-FdU_n conjugates were tested in (A) HCT116; (B) HCC2998; (C) HeLa and (D) Fibroblasts. Dotted line represents 50 % mortality (IC50). The most relevant estimated IC50 values are inserted in each panel and for more information see Supplementary Table S1. Error bars represent standard deviation (SD) of three independent experiments in triplicate. See Supplementary Fig. S20, S21, S22, and S23 for statistical differences.

also enables the conjugates to selectively target and kill cancer cells, thereby minimizing nonspecific adverse effects.

3.7. *INT aptamer with fluorine atoms improves cellular internalization*

Given the potential correlation between improved drug function and better internalization, we examined the cellular uptake of the aptamer-drug conjugate with the highest antiproliferative activity,

INT-FdU_{10} in comparison to the parent sequence INT and to the drug oligomer FdU_{10}. To follow the intracellular uptake, the oligonucleotides were labelled with fluorescein (FAM) at the 3′ end.

As expected, the cellular uptake is more efficient for all three tumor

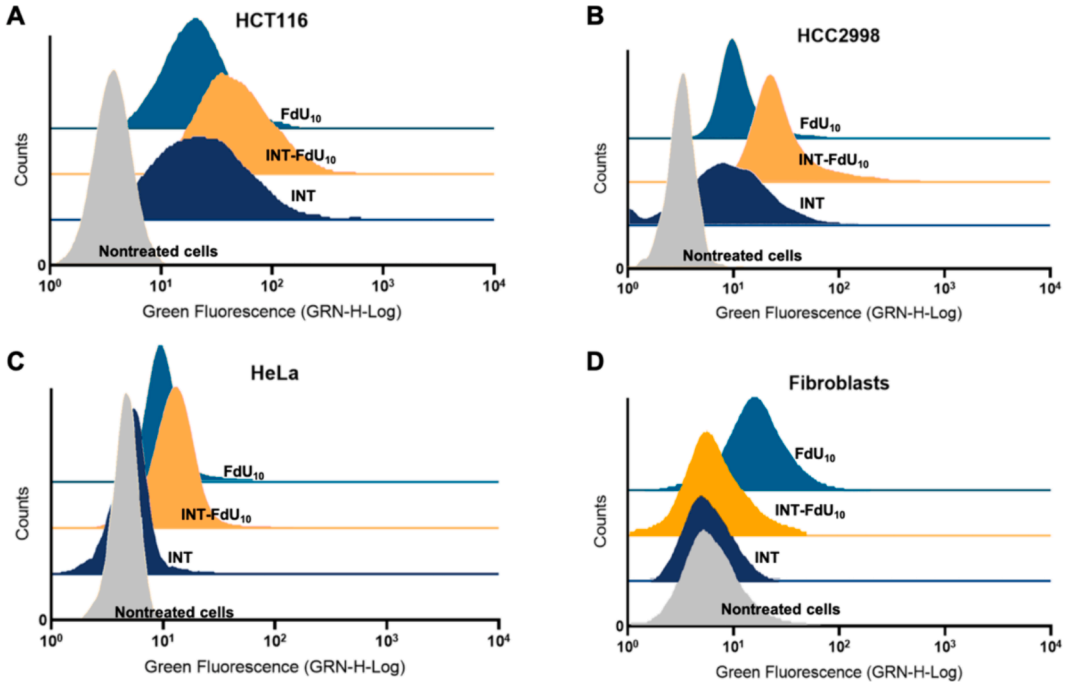

Fig. 5. Flow cytometry analysis of the uptake of INT, INT-FdU_{10}, FdU_{10} labeled with fluorescein by (A) HCT116; (B) HCC2998; (C) HeLa and (D) Fibroblasts cell lines. Nontreated cells were included as negative controls. The plots are the result of two independent experiments and each condition was measured in duplicate. See Supplementary Fig. S24 for statistical differences.

cell lines when INT is conjugated with FdU_{10} (Fig. 5 and Supplementary Fig. S24). Moreover, INT-FdU_{10} showed a better internalization than the control sequences INT with 10-thymidine tail (INT-T_{10}) and T_{10} (Supplementary Fig. S25) in agreement with previous studies suggesting that the presence of fluorine atoms in oligonucleotides improves internalization compared to non-fluorinated counterparts [39]. Notably, among the three cancer cell lines studied, HeLa cells exhibited the lowest internalization of INT conjugate, while HCT116 was the cell line in which it was more efficiently internalized implicating a potential difference in the number of G-quadruplex receptors between these two cancer cell lines. Our results also indicate that, despite INT and FdU_{10} being internalized similarly in terms of the percentage of cellular uptake, the two compounds exhibit different IC50 values, probably attributable to alternative mechanisms of action implied in cellular cytotoxicity.

Importantly, the cellular specificity was confirmed by differences in the efficiency between all tumor cell lines and fibroblasts. In good agreement with the MTT results, FdU_{10} is the only oligomer efficiently internalized in healthy cells. These data indicate that the internalization process of INT and the conjugate INT-FdU_{10} is more favorable in cancer cells due to the presence of the aptamer, which specifically facilitates the uptake of these compounds in tumor cells possibly through protein- and receptor-recognition [40–42].

Furthermore, we proceeded to examine INT and INT-FdU_{10} by fluorescence microscopy in HCT116, the cell line in which they showed higher internalization. Fluorescence microscopy images further confirmed the efficient internalization of both INT and INT-FdU_{10} in HCT116 (Fig. 6).

3.8. Endocytosis mechanisms

Once the efficiency of internalization of our compound in different cell lines was determined, we investigated the endocytosis mechanisms for the three tumor cell lines: HCT116, HCC2998, and HeLa. The objective was to identify the uptake pathways involved in this process, aiming to discern whether variations in the efficiency of internalization and cytotoxicity could be due to differences in endocytosis mechanisms. Cells were pretreated with compounds inhibiting specific endocytosis pathways: an inhibitor of clathrin-mediated endocytosis (sucrose), an inhibitor of caveolin-mediated endocytosis (Methyl-β-cyclodextrin), or an inhibitor of clathrin-independent endocytosis (lactose). After pretreatment, the cells were incubated with the corresponding INT, INT-FdU_{10}, or FdU_{10}, and the samples were analyzed by flow cytometry.

Interestingly, as shown in Fig. 7, the lack of inhibition of any endocytosis mechanism during FdU_{10} uptake suggests that, in all three cell lines, it undergoes internalization via gymnosis, as indicated in several previous studies [43]. Notably, the internalization mechanism of INT varies across cell lines. In HeLa, it is predominantly internalized through caveolin-mediated endocytosis, while in HCT116, it is clathrin-independent, and in HCC2998, it occurs through clathrin-mediated endocytosis. Conversely, INT-FdU_{10} exhibits internalization via caveolin-mediated endocytosis in HeLa, while in HCT116 and HCC2998, it is predominantly taken up through clathrin-mediated endocytosis. These findings are in good agreement with recent examples in the literature, indicating that the endocytic pathways involved in the internalization of the same compound are largely dependent on the cell type [44].

Moreover, results regarding endocytosis mechanisms are closely related to the cytotoxicity of the studied INT conjugates. When the aptamer or aptamer-drug conjugate is internalized through caveolin-dependent endocytosis, the cytotoxicity is higher, as it facilitates endosome escape, as demonstrated by the high cytotoxicity exhibited by all compounds in HeLa.

4. Conclusion

With the aim to enhance the therapeutic efficacy of the antineoplastic agent 5-fluoro-2′-deoxyuridine (FdU) and to minimize its off-target effects, we designed and synthesized three G4-aptamer/drug conjugates. In particular, the G4 forming aptamer T30923 (INT) was conjugated at the 3′ end with oligomers containing one, five, or ten units of FdU and the structural and biological properties of these compounds were analyzed. Similar to their unconjugated sequence, the resulting aptamer-drug conjugates showed the ability to fold into a dimeric G4 structure formed by the same G-quadruplexes, characterized by parallel strands, three all-anti-G-tetrads and three one-thymidine propeller loops.

Moreover, the unique stability against nucleases exhibited by this aptamer makes it highly promising as a vehicle for other drugs in future research. Interestingly cellular uptake data indicated that aptamer-drug conjugates are rapidly taken up by tumor cells, undergoing diverse endocytosis mechanisms. Unlike the G-quadruplex, the FdU oligomers are digested to release the active form of the drug, inhibiting proliferation in cancer cells, especially in HCT116 cells. The internalization

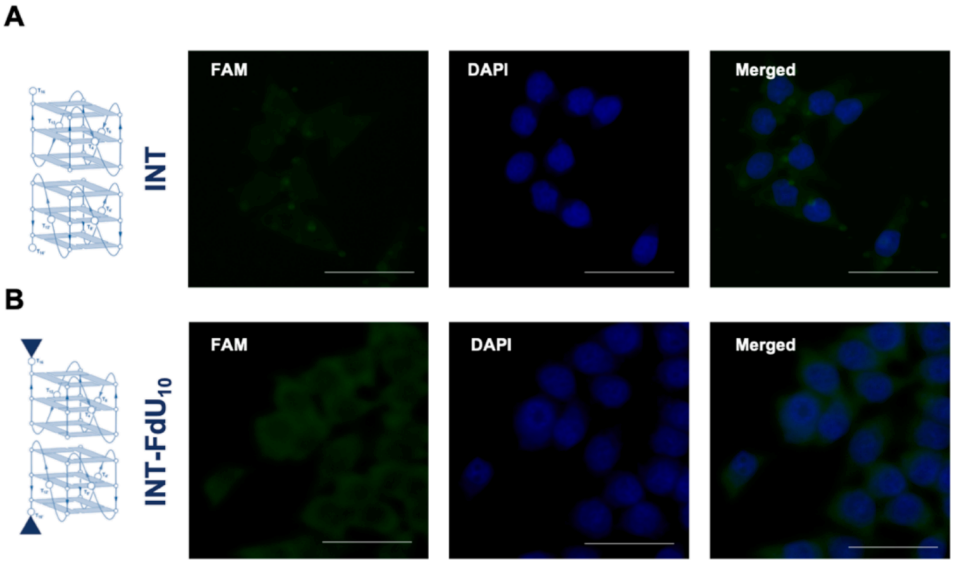

Fig. 6. Fluorescence microscopy images of cellular uptake of (A) INT and (B) INT-FdU_{10} in HCT116. Scale bar is 75 μm. Images are representative of several micrographs taken during independent experiments.

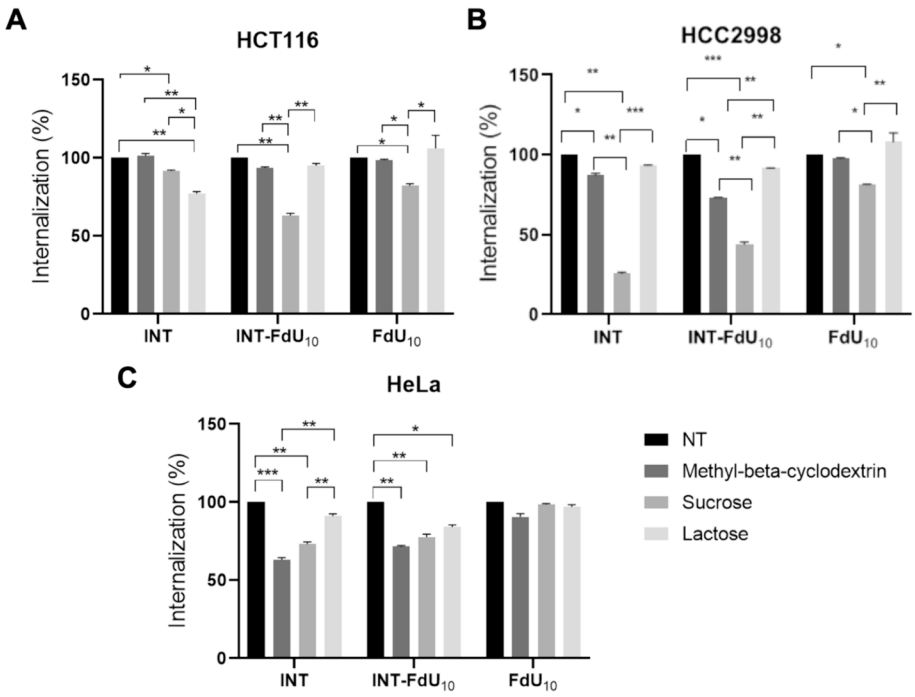

Fig. 7. Endocytosis pathways of INT, INT-FdU_{10}, FdU_{10} in cancer cells. Histogram analysis of the fluorescence signal of (A) HCT116; (B) HCC2998 and (C) HeLa cell lines treated with INT, INT-FdU_{10} and FdU_{10} in the presence of different endocytic inhibitors (shown in the legend). The relative cellular uptake efficiency was calculated by setting the signal of the cells treated with corresponding oligonucleotide in nontreated conditions (NT) as 100 %. Error bars represent standard deviation (SD) of two independent experiments in duplicate. One-way ANOVA with the Tukey post hoc test was applied for statistical differences (*$p \leq 0.0332$, **$p \leq 0.0021$, ***$p \leq 0.0002$, **** $p \leq 0.0001$).

process of INT and the conjugate INT-FdU_{10} is more favorable in cancer cells compared to healthy ones. Furthermore, in cancer cell lines the conjugates are internalized more effectively than the FdU_{10} oligomer alone. These data suggest that the aptamer specifically facilitates the uptake of these compounds in tumor cells possibly through protein- and receptor-recognition.

MTT assay performed on the oligomeric forms of FdU, INT and INT-FdU_n conjugates revealed that INT-FdU_{10} possesses the best antiproliferative activity in all cancer cell lines tested, but a lower cytotoxic activity in fibroblasts compared to unconjugated FdU oligomers.

In summary, the conjugation of the INT aptamer with antimetabolite nucleosides such as floxuridine results in a synergistic cytotoxic activity in tumor cells. Both compounds benefit from the antiproliferative characteristics and targeting capabilities for cancer treatment, avoiding side effects that may arise from the non-specificity and cellular resistance of FdU alone or enhancing the efficacy of the INT aptamer by conjugating it with an FdU tail, thereby increasing its antiproliferative activity. In the future, aptamer-drug conjugates may be expanded to other tumor-targeting aptamer sequences and/or conjugated with other antitumor drugs. Aptamer-drug conjugates are easy to synthesize, have precise and simple structures and high targeting capabilities which may expand their scope for novel and improved cancer therapies.

Funding

This work was financially supported by the Spanish Ministerio de Ciencia e Innovación (MICINN) [Project PID2020-118145RB-I00] and Funded by the European Union-NextGenerationEU - PNRR MUR - PRIN 2022 – [CUP UNINA: E53D23009940006]. N.N. held a predoctoral contract grant [PRE2021-097856]. This research was also supported by CIBER - Consorcio Centro de Investigación Biomédica en Red [CB06/01/0019], Instituto de Salud Carlos III, Ministerio de Ciencia e Innovación, European Regional Development Fund (ERDF) and University of Naples Federico II.

CRediT authorship contribution statement

Daniela Benigno: Writing – review & editing, Writing – original draft, Validation, Methodology, Investigation, Data curation. **Natalia Navarro:** Writing – review & editing, Writing – original draft, Validation, Supervision, Methodology, Investigation. **Anna Aviñó:** Writing – review & editing, Investigation. **Veronica Esposito:** Writing – review & editing, Supervision, Funding acquisition, Conceptualization. **Aldo Galeone:** Writing – review & editing, Supervision, Funding acquisition, Conceptualization. **Antonella Virgilio:** Writing – review & editing, Supervision, Funding acquisition, Conceptualization. **Carme Fàbrega:** Writing – review & editing, Writing – original draft, Validation, Supervision, Methodology, Funding acquisition, Data curation, Conceptualization. **Ramon Eritja:** Writing – review & editing, Supervision, Funding acquisition, Conceptualization.

Declaration of competing interest

The authors declare that they have no known competing financial interests or personal relationships that could have appeared to influence the work reported in this paper.

Data availability

Data will be made available on request.

All data generated or analyzed during this study are included in this published article and its supplementary information files.

Acknowledgements

We acknowledge Dr. Mireia Casasampere and Prof. Gemma Fabriàs for kindly providing HCT116 and Fibroblasts cell lines. We also thank Arnau Domínguez for assistance with oligonucleotides synthesis and CD measurements. Oligonucleotide synthesis was performed by the ICTS

"NANBIOSIS" and specifically by the oligonucleotide synthesis platform (OSP) U29 at IQAC-CSIC (https://www.nanbiosis.es/portfolio/u29-oligonucleotide-synthesis-platform-osp/).

Appendix A. Supplementary material

Supplementary data to this article can be found online at https://doi.org/10.1016/j.ejpb.2024.114354.

References

[1] M. Srinivasarao, P.S. Low, Ligand-Targeted Drug Delivery, Chem. Rev. 117 (2017) 12133–12164, https://doi.org/10.1021/acs.chemrev.7b00013.

[2] J.L. Grem, 5-Fluorouracil: Forty-Plus and Still Ticking, A Review of Its Preclinical and Clinical Development, Invest New Drugs 18 (2000) 299–313, https://doi.org/10.1023/A:1006416410198.

[3] J.A.M. van Laar, Y.M. Rustum, S.P. Ackland, C.J. van Groeningen, G.J. Peters, Comparison of 5-fluoro-2′-deoxyuridine with 5-fluorouracil and their role in the treatment of colorectal cancer, Eur. J. Cancer 34 (1998) 296–306, https://doi.org/10.1016/S0959-8049(97)00366-3.

[4] D.B. Longley, D.P. Harkin, P.G. Johnston, 5-fluorouracil: mechanisms of action and clinical strategies, Nat. Rev. Cancer 3 (2003) 330–338, https://doi.org/10.1038/nrc1074.

[5] A.F. Jorge, A. Aviñó, A.A.C.C. Pais, R. Eritja, C. Fàbrega, DNA-based nanoscaffolds as vehicles for 5-fluoro-2′-deoxyuridine oligomers in colorectal cancer therapy, Nanoscale 10 (2018) 7238–7249, https://doi.org/10.1039/c7nr08442k.

[6] N. Navarro, A. Aviñó, Ò. Domènech, J.H. Borrell, R. Eritja, C. Fàbrega, Defined covalent attachment of three cancer drugs to DNA origami increases cytotoxicity at nanomolar concentration, Nanomedicine 55 (2024) 102722, https://doi.org/10.1016/j.nano.2023.102722.

[7] A. Aviñó, A. Clua, M.J. Bleda, R. Eritja, C. Fàbrega, Evaluation of floxuridine oligonucleotide conjugates carrying potential enhancers of cellular uptake, Int. J. Mol. Sci. 22 (2021), https://doi.org/10.3390/ijms22115678.

[8] M.V. Céspedes, U. Unzueta, A. Aviñó, A. Gallardo, P. Álamo, R. Sala, A. Sánchez-Chardi, I. Casanova, M.A. Mangues, A. Lopez-Pousa, R. Eritja, A. Villaverde, E. Vázquez, R. Mangues, Selective depletion of metastatic stem cells as therapy for human colorectal cancer, EMBO Mol. Med. 10 (2018), https://doi.org/10.15252/emmm.201708772.

[9] S. Kruspe, U. Hahn, An Aptamer Intrinsically Comprising 5-Fluoro-2′-deoxyuridine for Targeted Chemotherapy, Angewandte Chemie - International Edition 53 (2014) 10541–10544, https://doi.org/10.1002/anie.201405778.

[10] L. Zhu, J. Yang, Y. Ma, X. Zhu, C. Zhang, Aptamers Entirely Built from Therapeutic Nucleoside Analogues for Targeted Cancer Therapy, J. Am. Chem. Soc. 144 (2022) 1493–1497, https://doi.org/10.1021/jacs.1c09574.

[11] Y. Zhan, W. Ma, Y. Zhang, C. Mao, X. Shao, X. Xie, F. Wang, X. Liu, Q. Li, Y. Lin, DNA-Based Nanomedicine with Targeting and Enhancement of Therapeutic Efficacy of Breast Cancer Cells, ACS Appl. Mater. Interfaces 11 (2019) 15354–15365, https://doi.org/10.1021/acsami.9b03449.

[12] S. Yoon, K.W. Huang, V. Reebye, D. Spalding, T.M. Przytycka, Y. Wang, P. Swiderski, L. Li, B. Armstrong, I. Reccia, D. Zacharoulis, K. Dimas, T. Kusano, J. Shively, N. Habib, J.J. Rossi, Aptamer-Drug Conjugates of Active Metabolites of Nucleoside Analogs and Cytotoxic Agents Inhibit Pancreatic Tumor Cell Growth, Mol. Ther. Nucleic Acids 6 (2017) 80–88, https://doi.org/10.1016/j.omtn.2016.11.008.

[13] Y. Li, J. Zhao, Z. Xue, C. Tsang, X. Qiao, L. Dong, H. Li, Y. Yang, B. Yu, Y. Gao, Aptamer nucleotide analog drug conjugates in the targeting therapy of cancers, Front. Cell Dev. Biol. 10 (2022), https://doi.org/10.3389/fcell.2022.1053984.

[14] Y. Xu, X. Jiang, Y. Zhou, M. Ma, M. Wang, B. Ying, Systematic Evolution of Ligands by Exponential Enrichment Technologies and Aptamer-Based Applications: Recent Progress and Challenges in Precision Medicine of Infectious Diseases, Front. Bioeng. Biotechnol. 9 (2021), https://doi.org/10.3389/fbioe.2021.704077.

[15] M.H. Ali, M.E. Elsherbiny, M. Emara, Updates on Aptamer Research, Int. J. Mol. Sci. 20 (2019) 2511, https://doi.org/10.3390/ijms20102511.

[16] K.-M. Song, S. Lee, C. Ban, Aptamers and Their Biological Applications, Sensors 12 (2012) 612–631, https://doi.org/10.3390/s120100612.

[17] G. Zhu, G. Niu, X. Chen, Aptamer-Drug Conjugates, Bioconjug. Chem. 26 (2015) 2186–2197, https://doi.org/10.1021/acs.bioconjchem.5b00291.

[18] C. Roxo, W. Kotkowiak, A. Pasternak, G-Quadruplex-Forming Aptamers—Characteristics, Applications, and Perspectives, Molecules 24 (2019) 3781, https://doi.org/10.3390/molecules24203781.

[19] S. Burge, G.N. Parkinson, P. Hazel, A.K. Todd, S. Neidle, Quadruplex DNA: sequence, topology and structure, Nucleic Acids Res. 34 (2006) 5402–5415, https://doi.org/10.1093/nar/gkl655.

[20] A.N. Lane, J.B. Chaires, R.D. Gray, J.O. Trent, Stability and kinetics of G-quadruplex structures, Nucleic Acids Res. 36 (2008) 5482–5515, https://doi.org/10.1093/nar/gkn517.

[21] J. Eddy, N. Maizels, Gene function correlates with potential for G4 DNA formation in the human genome, Nucleic Acids Res. 34 (2006) 3887–3896, https://doi.org/10.1093/nar/gkl529.

[22] C. Platella, C. Riccardi, D. Montesarchio, G.N. Roviello, D. Musumeci, G-quadruplex-based aptamers against protein targets in therapy and diagnostics, Biochimica et Biophysica Acta (BBA) - General Subjects 1861 (2017) 1429–1447. DOI: 10.1016/j.bbagen.2016.11.027.

[23] A.M. Ogloblina, A.N. Khristich, N.Y. Karpechenko, S.E. Semina, G.A. Belitsky, N. G. Dolinnaya, M.G. Yakubovskaya, Multi-targeted effects of G4-aptamers and their antiproliferative activity against cancer cells, Biochimie 145 (2018) 163–173, https://doi.org/10.1016/j.biochi.2017.11.020.

[24] R. Yazdian-Robati, P. Bayat, F. Oroojalian, M. Zargari, M. Ramezani, S.M. Taghdisi, K. Abnous, Therapeutic applications of AS1411 aptamer, an update review, Int. J. Biol. Macromol. 155 (2020) 1420–1431, https://doi.org/10.1016/j.ijbiomac.2019.11.118.

[25] P. Weerasinghe, G.E. Garcia, Q. Zhu, P. Yuan, L. Feng, L. Mao, N. Jing, Inhibition of Stat3 activation and tumor growth suppression of non-small cell lung cancer by G-quartet oligonucleotides, Int. J. Oncol. 31 (2007) 129–136.

[26] V. Esposito, D. Benigno, I. Bello, E. Panza, M. Bucci, A. Virgilio, A. Galeone, Structural and Biological Features of G-Quadruplex Aptamers as Promising Inhibitors of the STAT3 Signaling Pathway, Int. J. Mol. Sci. 24 (2023), https://doi.org/10.3390/ijms24119524.

[27] N. Jing, C. Marchand, J. Liu, R. Mitra, M.E. Hogan, Y. Pommier, Mechanism of Inhibition of HIV-1 Integrase by G-tetrad-forming Oligonucleotides in Vitro, J. Biol. Chem. 275 (2000) 21460–21467, https://doi.org/10.1074/jbc.M001436200.

[28] V. Esposito, L. Pirone, L. Mayol, E. Pedone, A. Virgilio, A. Galeone, Exploring the binding of d(GGGT)4 to the HIV-1 integrase: An approach to investigate G-quadruplex aptamer/target protein interactions, Biochimie 127 (2016) 19–22, https://doi.org/10.1016/j.biochi.2016.04.013.

[29] V. Esposito, F. Esposito, A. Pepe, I.G. Monterrey, E. Tramontano, L. Mayol, A. Virgilio, A. Galeone, Probing the importance of the g-quadruplex grooves for the activity of the anti-hiv-integrase aptamer t30923, Int. J. Mol. Sci. 21 (2020) 1–13, https://doi.org/10.3390/ijms21165637.

[30] E. Magbanua, T. Zivkovic, N. Björn Hansen, C. Beschorner, I.L. Meyer, J. Joachim Grötzinger, A.E.T. Hauber, S. Günter Mayer, U.H. Rose-John, D(GGGT)4 and r(GGGU)4 are both HIV-1 inhibitors and interleukin-6 receptor aptamers, RNA Biol. 10 (2013) 216–227, https://doi.org/10.4161/rna.22951.

[31] V. Dapić, V. Abdomerović, R. Marrington, J. Peberdy, A. Rodger, J.O. Trent, P. J. Bates, Biophysical and biological properties of quadruplex oligodeoxyribonucleotides, Nucleic Acids Res. 31 (2003) 2097–2107, https://doi.org/10.1093/nar/gkg316.

[32] N. Jing, Y. Li, X. Xu, W. Sha, P. Li, L. Feng, D.J. Tweardy, Targeting Stat3 with G-Quartet Oligodeoxynucleotides in Human Cancer Cells, DNA Cell Biol. 22 (2003) 685–696, https://doi.org/10.1089/104454903770946665.

[33] A. Virgilio, A. Pecoraro, D. Benigno, A. Russo, G. Russo, V. Esposito, A. Galeone, Antiproliferative Effects of the Aptamer d(GGGT)4 and Its Analogues with an Abasic-Site Mimic Loop on Different Cancer Cells, Int. J. Mol. Sci. 23 (2022), https://doi.org/10.3390/ijms23115952.

[34] N.Q. Do, K.W. Lim, M.H. Teo, B. Heddi, A.T. Phan, Stacking of G-quadruplexes: NMR structure of a G-rich oligonucleotide with potential anti-HIV and anticancer activity, Nucleic Acids Res. 39 (2011) 9448–9457, https://doi.org/10.1093/nar/gkr539.

[35] A. Clua, C. Fàbrega, J. García-Chica, S. Grijalvo, R. Eritja, Parallel G-quadruplex structures increase cellular uptake and cytotoxicity of 5-fluoro-2'-deoxyuridine oligomers in 5-fluorouracil resistant cells, Molecules 26 (2021), https://doi.org/10.3390/molecules26061741.

[36] W.H. Gmeiner, W. Debinski, C. Milligan, D. Caudell, T.S. Pardee, The applications of the novel polymeric fluoropyrimidine F10 in cancer treatment: current evidence, Future Oncol. 12 (2016) 2009–2020, https://doi.org/10.2217/fon-2016-0091.

[37] T.L. Hwang, A.J. Shaka, Water Suppression That Works, Excitation Sculpting Using Arbitrary Wave-Forms and Pulsed-Field Gradients, J Magn Reson A 112 (1995) 275–279, https://doi.org/10.1006/jmra.1995.1047.

[38] J.M. Mariadason, D. Arango, Q. Shi, A.J. Wilson, G.A. Corner, C. Nicholas, M. J. Aranes, M. Lesser, E.L. Schwartz, L.H. Augenlicht, Gene expression profiling-based prediction of response of colon carcinoma cells to 5-fluorouracil and camptothecin, Cancer Res. 63 (2003) 8791–8812.

[39] N. Navarro, S. Serantes, A. Aviñó, C. Fàbrega, R. Eritja, Synthesis and Evaluation of 3′-Oleyl–Oligonucleotide Conjugates as Potential Cellular Uptake Enhancers, Synlett (2023), https://doi.org/10.1055/s-0042-1751528.

[40] J. Lopes-Nunes, P. Oliveira, C. Cruz, G-Quadruplex-Based Drug Delivery Systems for Cancer Therapy, Pharmaceuticals 14 (2021) 671, https://doi.org/10.3390/ph14070671.

[41] X. Song, H. Yu, C. Sullenger, B.P. Gray, A. Yan, L. Kelly, B. Sullenger, An Aptamer That Rapidly Internalizes into Cancer Cells Utilizes the Transferrin Receptor Pathway, Cancers (basel) 15 (2023) 2301, https://doi.org/10.3390/cancers15082301.

[42] S. Kitagawa, T. Matsuda, A. Washizaki, H. Murakami, T. Yamamoto, Y. Yoshioka, Elucidation of the role of nucleolin as a cell surface receptor for nucleic acid-based adjuvants, npj Vaccines 7 (2022) 115, https://doi.org/10.1038/s41541-022-00541-6.

[43] C. Fàbrega, A. Clua, R. Eritja, A. Aviñó, oligonucleotides carrying nucleoside antimetabolites as potential prodrugs, Curr. Med. Chem. 30 (2023) 1304–1319, https://doi.org/10.2174/0929867328666211129124039.

[44] A. Rajwar, S.R. Shetty, P. Vaswani, V. Morya, A. Barai, S. Sen, M. Sonawane, D. Bhatia, Geometry of a DNA Nanostructure Influences Its Endocytosis: Cellular Study on 2D, 3D, and *in Vivo* Systems, ACS Nano 16 (2022) 10496–10508, https://doi.org/10.1021/acsnano.2c01382.